Geochemical Journal, Vol. 49, pp. 63 to 71, 2015 doi:10.2343/geochemj.2.0331

Variations in soil organic carbon contents and isotopic compositions under different land uses in a typical karst area in Southwest China

GUILIN HAN,[1]* FUSHAN LI[2,3] and YANG TANG[2]

[1]School of Water Resources and Environment, China University of Geosciences (Beijing), Beijing 10083, China
[2]The State Laboratory of Environmental Geochemistry, Institute of Geochemistry, Chinese Academy of Sciences, Guiyang 550002, China
[3]University of Chinese Academy of Sciences, Beijing 100049, China

(*Received March 21, 2014; Accepted September 4, 2014*)

Land use changes can affect soil carbon storage in terrestrial ecosystems by altering either the biotic or the abiotic processes involved in carbon cycling, such as the adsorption of carbon on soil minerals. In this study, the organic carbon contents and their stable carbon isotopic compositions ($\delta^{13}C$) of five soil profiles under different land uses in the Maolan karst region in Southwest China were analyzed. Four non-forest samples from the karst were selected and examined to determine whether farmlands or grasslands that were converted from forestland were more effective in sequestering carbon in soils. The soil organic carbon (SOC) contents decreased in the following order: virgin forest, burnt grassland, shrubland, grassland, and farmland. However, no differences were observed in the $\delta^{13}C$ values at the bottom of the five profiles, which indicated that most of the soil organic carbon was derived from the original virgin forest. The percentages of SOC that resulted from C_4 plants in the virgin forest were significantly lower than the percentages in the other plots, while the percentages of SOC that resulted from C_3 plants in the virgin forest were significantly higher than the percentages in the other plots. The $\delta^{13}C$ values in the topsoils of the various profiles decreased in the following order: burnt grassland, farmland, grassland, shrubland, and virgin forest. From the surface to the base of the farmland profiles, little variation occurred in the $\delta^{13}C$ values of the SOC (from –25.1 to –29.1‰). This variation in the $\delta^{13}C$ values of the SOC in the surface soils was associated with changes in the vegetation cover. In addition, our results suggest that the plant functional type is important for controlling the depth-related changes in the SOC contents and the $\delta^{13}C$ values of the SOC.

Keywords: soil organic carbon, stable carbon isotope, karst areas, Southwest China

INTRODUCTION

Soil is the largest pool of terrestrial organic carbon in the biosphere. Soil stores more carbon than plants and the atmosphere combined (Malhi *et al*., 1999). The abundance of organic carbon in the soil affects and is affected by plant production. In addition, the roles of organic carbon in soil fertility and agricultural production have been recognized for more than a century (Jobbagy and Jackson, 2000). It is important to identify the patterns and controls of soil organic carbon (SOC) storage to understand how SOC is important in ecosystem processes and is directly linked to atmospheric composition and climate change (Raich and Potter, 1995; Trumbore *et al*., 1996; Woodwell *et al*., 1998; Jobbagy and Jackson, 2000; Feng *et al*., 2010). SOC storage is controlled by balancing carbon inputs from plant photosynthesis and carbon outputs from decomposition (Schlesinger, 1977). Although climate and soil texture are the primary regional controls of SOC storage, their influences on the vertical distribution of SOC may be outweighed by the effects of changing land use and vegetation cover (Jabbagy and Jackson, 2000).

The impacts of human activities and land use changes, such as deforestation and cultivation, on the structural and functional properties of an ecosystem can be studied using stable isotopes (Boutton *et al*., 1998; Staddon, 2004). The naturally occurring $\delta^{13}C$ values of biologically interesting carbon compounds vary from approximately 0 to –110‰ relative to the Pee Dee Belemnite standard (Vagen *et al*., 2006). C_3 plants use the Calvin-Benson photosynthetic pathway (Calvin and Benson, 1948) and fractionate carbon differently than do C_4 plants, which use the Hatch-Slack pathway (Hatch and Slack, 1970). In C_3 plants, CO_2 is reduced to a three-carbon compound. The $\delta^{13}C$ values of C_3 plants are generally between –33‰ and –22‰, with a mean of –27‰ for woody plants (Vagen *et al*., 2006). However, C_4 plants reduce CO_2 to a four-carbon compound and have $\delta^{13}C$ values of

*Corresponding author (e-mail: hanguilin@cugb.edu.cn)

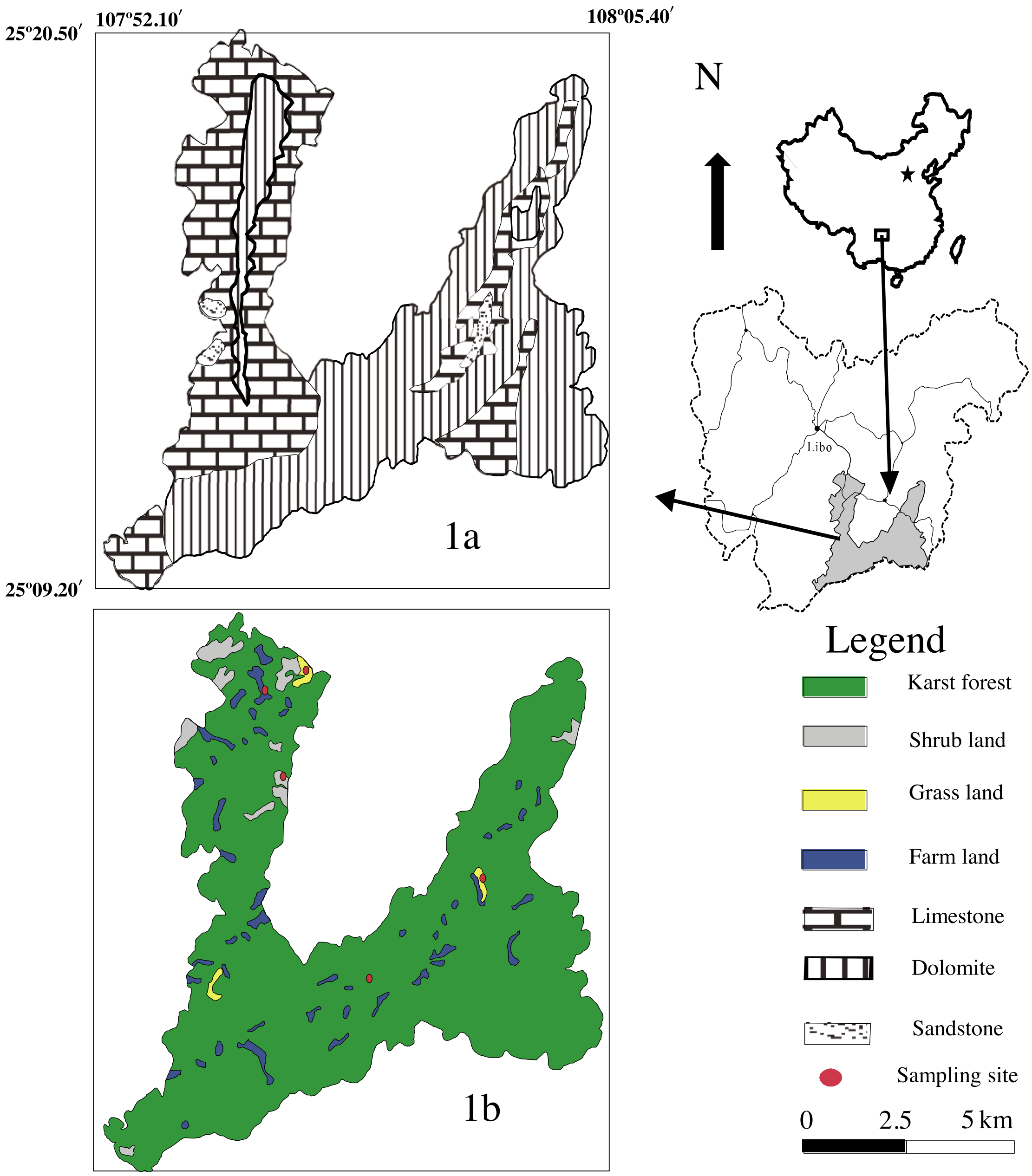

Fig. 1. Map showing the lithology and land uses in the Maolan National Nature Reserved Park.

–17‰ to –9‰, with a mean of –14‰ (Boutton *et al.*, 1998). These differences occur because C_3 plants discriminate more heavily against the heavier isotope than do C_4 plants. The utility of $\delta^{13}C$ isotopic tracers for soil organic matter (SOM) studies stems from the fact that all plants discriminate against $\delta^{13}C$ during photosynthesis, but at different degrees depending on their photosynthetic pathway (Farquhar *et al.*, 1989).

Soil degradation is the main cause of land degradation (Raich and Potter, 1995). Soil organic matter plays important roles in soil degradation and in the global carbon cycle. In addition, soil is an important element in karst processes and karst ecosystems (Wang *et al.*, 1999), with soil organic matter and soil microorganisms significantly reducing the rates of limestone erosion (Li *et al.*, 2004). Regional rock desertification is a serious ecological problem in the subtropical karst regions of Southwest China because it results in the progressive impoverishment of local residents, and rock desertification is a process of land degradation resulting from the comprehensive action due to the overprint of irrational anthropological activities on the karst fragile environment (Yuan, 1997). As part of the ongoing research of rock desertification and the rehabilitation of karst ecosystems, increasing attention has been directed to the interactions between human activities and natural karst systems, especially the effects of land use cover on natural systems (Zhang and Yuan, 2004).

However, little research has been conducted regarding the changes in the stable carbon isotopic compositions of modern soils at different depths and under different types of land use in karst areas (Zhu and Liu, 2006). This study examines the depth profiles of SOC and $\delta^{13}C$ in five plots with differing vegetation cover in a typical karst area in Southwest China. The nature of plant cover (forest, grass, crops) affects pedogenetic weathering and changes the soil organic matter properties. Thus, we aimed to determine the potential effects of vegetation changes on soil carbon storage in a typical karst ecosystem in order to clarify the relationships between dominant vegetation types and the vertical distribution of SOC and stable carbon isotopes. In addition, this study aimed to provide fundamental information to support the protection of fragile soil resources and adjust land use structures in Maolan, Southwest China.

Materials and Methods

Study area

The Maolan National Nature Reserve Park in the southeastern region of Guizhou Province, Southwest China, is famous for its dense virgin evergreen forests, which grow on the peak cluster karst. Our study sites are located between latitudes of 25°09′20″N and 25°20′50″N and longitudes of 107°52′10″E and 108°05′40″E (Fig. 1). The climate in this region is subtropical, monsoon, and humid, with a mean annual temperature of 17°C and a mean annual precipitation of 1750 mm. The rock exposures in the study area are sedimentary formations of limestone, dolomite, sandstone, and clay of the Middle to Lower Carboniferous period (Fig. 1a).

Soil samples were collected from the park to represent chronosequences of deforestation and land use changes. The reserve covers an area of *ca*. 200 km^2, consisting mostly of mountains of jagged carbonate rocks with 90% forest cover (Fig. 1b). The sampling strategy was designed to collect representative data from various landforms, land use types, and areas with different conversion histories to cover a range of soil conditions. The sampling areas were selected based on field surveys and interviews with farmers and local experts. Five types of soil profiles were chosen for sampling during the summer of 2007. In addition to the virgin forest site, one sample site was converted to intensive maize cropping, one site was converted to shrubland, and two sites were converted to grassland in recent decades. The visible charac-

Table 1. Visible characteristic of the five soil profiles

Profile	Profile thickness (cm)	Dominant vegetable species	Visible characteristics
Profile of grass land (GL)	110	dominated by C_4 vegetation: *Miscanthus floridulus; Imperata cylindrical*	0–20 cm: black, humus layer, abundant plant roots 20–110 cm: yellow, clayey
Profile of shrub land (SL)	90	dominated by: *Pyracantha fortuneana* (C_3); *Quercus glauca* (C_4)	0–20 cm: black, humus layer, abundant plant roots 20–90 cm: brawn to yellow soil
Profile of farm land (FL)	110	dominated by: *Zea mays* (C_4)	0–90 cm: black, clayey, tight, no rootlets 90–110 cm: yellow, tight, merges to weathering rock below
Profile of burnt grass land (BGL)	70	dominated by C_4 vegetation: *Miscanthus floridulus; Imperata cylindrical*	0–20 cm: black, humus layer, abundant plant roots 20–70 cm: yellow limestone soil
Profile of virgin forest land (VFL)	120	Dominated by C_3 vegetation: *Rosacym osa; Lindera communis; Pyracantha fortuneana; Selaginella tamariscina; Castanopsis tibetana*	0–20 cm: black, humus layer, abundant plant roots 20–120 cm: black brawn to yellow brown, visible plant roots, clayey

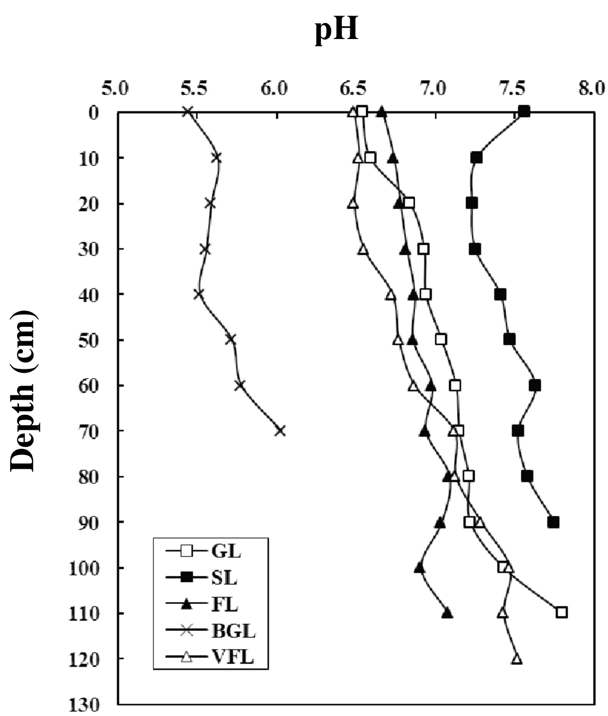

Fig. 2. Changes in soil pH with depth in the five soil profiles.

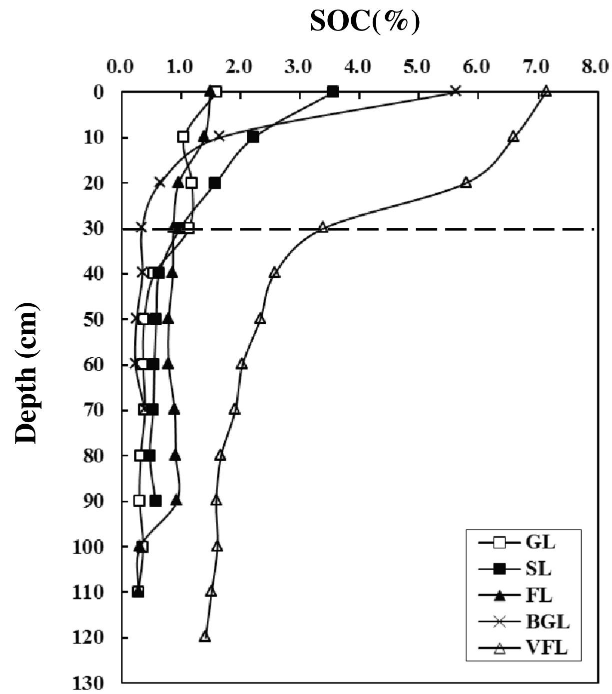

Fig. 3. Changes in soil organic carbon with depth in the five soil profiles.

teristics of the studied profiles are summarized in Table 1. The grassland (GL), shrubland (SL), burnt grassland (BGL), and virgin forestland (VFL) species profiles mainly contained C_3 plants. Maize, an important food crop that uses C_4-photosynthesis, was grown in the farmland (FL) profile.

Soil sampling and analysis

Three soil profiles were chosen under each type of land use. At each site, soil samples were collected at intervals of 10 cm to a depth of up to 120 cm from the walls of the soil pits (Table 1). The three soil profiles under the same land uses were very similar (data not shown), therefore, the authors chose the longest profiles under the different vegetation covers for further discussion. Soil samples were air dried and then sufficiently disaggregated by passing through a 2 mm sieve.

Soil samples were treated with 0.5 mol/L HCl at 25°C for 24 h to remove carbonates (Midwood and Boutton, 1998) before washing to neutrality with distilled water, centrifuging and drying at 60°C. Next, the samples were pulverized and saved for carbon and isotopic analyses.

Soil pH was measured using a glass electrode in a 1:2.5 soil:water suspension (Liu *et al.*, 1996) with a precision of ±0.05. The organic carbon content was analyzed by combustion using an elemental analyzer (PE2400, Perkin Elmer, USA) with a precision of ≤0.1%.

For the stable isotopic analysis, a sample mass yielding 0.5 mg of carbon was placed in a quartz tube with CuO and Pt wire. Next, the sample tube was evacuated and flame sealed. The organic carbon in the sample was oxidized to CO_2 at 850°C for 5 h. CO_2 was collected and purified cryogenically in a vacuum extraction line, and the quantity of CO_2 was measured before collecting it in the break-seal tube for subsequent mass spectrometric analysis (Boutton *et al.*, 1983). The stable carbon isotope ratios ($^{13}C/^{12}C$) were measured using a mass spectrometer (MAT-252, Finnigan MAT, USA). The carbon isotope values in this study are reported using the δ notation relative to international standard; Pee Dee Belemnite (PDB):

$$\delta^{13}C(‰) = [(R_{sample} - R_{PDB})/R_{PDB}] \times 1000,$$

where $R = {}^{13}C/{}^{12}C$.

Routine $\delta^{13}C$ measurements were conducted with an overall precision of ±0.1‰. Isotopic standards of carbonate and IAEA-C3 (cellulose) were repeatedly measured to determine the reproducibility of the analyses. Each sample was run in duplicate, and the results indicated that the differences were less than the range of measurement accuracy.

Calculation and data analyses

The proportion of past C_4 versus C_3 vegetation is often calculated using the δ^{13}C values of SOC in a simple mass balance mixing formula (Resh *et al.*, 2002; Biedenbender *et al.*, 2004; Li and Mathews, 2010).

$$\delta^{13}C_{sample} = x\delta^{13}C_4 + (1 - x)\delta^{13}C_3.$$

This two-end-member model can be used where the dominant photosynthetic pathway of the plant community has changed. In this case, $\delta^{13}C_{sample}$ is the δ^{13}C value of the soil sample, x corresponds with the percentage of SOC that results from the previous C_4 vegetation, $\delta^{13}C_3$ is the δ^{13}C value of the C_3 vegetation, and $\delta^{13}C_4$ is the δ^{13}C value of the C_4 vegetation.

$$x = [\ (\delta^{13}C_{sample} - \delta^{13}C_3)/(\delta^{13}C_4 - \delta^{13}C_3)].$$

In this case, $\delta^{13}C_3$ is the average δ^{13}C value of the forest litter, stems, and roots in the Maolan areas (–29.1‰, Piao *et al.*, 2001), and $\delta^{13}C_4$ is the average δ^{13}C value of the maize litter, stems, and roots in the Maolan areas (–11.4‰, Piao *et al.*, 2001). These calculations were based on the assumption that most virgin forests are composed of C_3 vegetation. However, some of the understory vegetation is composed of C_4 vegetation (most grasses, including maize, are C_4 species).

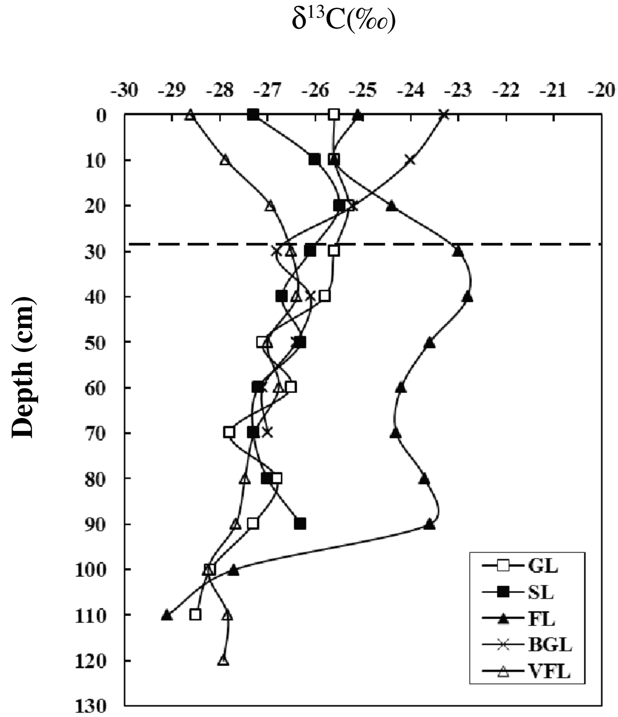

Fig. 4. Vertical patterns of the stable carbon isotope (δ^{13}C) in the bulk soil from the five soil profiles.

Results

Soil pH

The soils from the five land use types had different pH values (Fig. 2), but the pH generally increased with soil depth in all types. The soil samples in the SL profile had relatively high pH values that varied from 7.2 at the surface to 7.8 at the base. The pH ranges in the GL, FL, and VFL profiles were 6.5 to 7.8, 6.7 to 7.1, and 6.7 to 7.5, respectively. The BGL profile had the lowest pH values of 5.5 to 6.0.

SOC content

The SOC contents exceeded 1.0% in all of the horizons of the five profiles, with a maximum value of 7.1% (the topsoil in the VFL profile). The SOC contents in the VFL profile were distinctly different from the contents in the FL profile, and the soils in the GL and FL profiles were characterized by relatively low surface SOC contents of 1.59% and 1.49%, respectively (Fig. 3). The highest SOC content (7.1%) was recorded in the VFL profile, and the SOC contents in the SL and BGL profiles were 3.56% and 5.63%, respectively. The change in the SOC content with depth was categorized by two soil layers in each of the five soil profiles (Fig. 3). From the maximal SOC contents in the topsoil, the SOC content decreased exponentially with depth before decreasing more slowly below a certain depth (approximately 30 cm) and becoming more or less stable in the deepest layer. However, the rate of the decrease and the thickness of the surface soil layer were different in each profile. The rate of decreasing SOC with depth in the BGL profile was greater than the rate observed in the other profiles. The VFL profile had the highest SOC content, and the other sites were ranked as follows: $SOC_{VFL} > SOC_{BGL} > SOC_{SL} > SOC_{GL} > SOC_{FL}$.

Stable carbon isotopic composition of the soil

The δ^{13}C values of the topsoil from the GL, SL, FL, BGL and VFL profiles were –25.6‰, –27.3‰, –25.1‰, –23.3‰ and –28.6‰, respectively (Fig. 4). The δ^{13}C values of the VFL showed no significant changes with depth. The δ^{13}C values of soil samples from GL, SL, BGL, and FL profiles gradually decreased with depth when compared with the surface horizons. The greatest enrichment of ^{12}C occurred at the bottoms of the profiles.

The δ^{13}C values of the soils in all of the profiles changed with depth from 0–30 cm, but the values of all profiles decreased gradually below 30 cm with depth (Fig. 4). The δ^{13}C values did not increase continuously with depth in the FL and VFL profiles, but reached a maximum at a certain depth (30 cm) before gradually decreasing. From the topsoil to 30 cm, the δ^{13}C values of the

Table 2. The pH values, percentages (%) of SOC and $\delta^{13}C$ of soil organic carbon in different profiles

Depth (cm)	GL				SL				FL				BGL				VFL			
	pH	SOC (%)	$\delta^{13}C$ (‰)	SOC_4 (%)	pH	SOC (%)	$\delta^{13}C$ (‰)	SOC_4 (%)	pH	SOC (%)	$\delta^{13}C$ (‰)	SOC_4 (%)	pH	SOC (%)	$\delta^{13}C$ (‰)	SOC_4 (%)	pH	SOC (%)	$\delta^{13}C$ (‰)	SOC_4 (%)
0	6.54	1.59	−25.6	20	7.56	3.56	−27.3	10	6.67	1.49	−25.1	23	5.45	5.63	−23.3	33	6.49	7.13	−28.6	3
10	6.59	1.05	−25.6	20	7.26	2.22	−26.0	18	6.74	1.39	−25.6	20	5.63	1.64	−24.0	29	6.52	6.59	−27.9	7
20	6.84	1.18	−25.3	22	7.23	1.58	−25.5	20	6.78	0.96	−24.4	27	5.59	0.65	−25.2	22	6.49	5.79	−26.9	12
30	6.93	1.13	−25.6	20	7.25	0.98	−26.1	17	6.82	0.87	−23.0	35	5.56	0.34	−26.8	13	6.55	3.39	−26.5	15
40	6.94	0.55	−25.8	19	7.41	0.63	−26.7	14	6.87	0.86	−22.8	36	5.52	0.35	−26.1	17	6.73	2.57	−26.4	15
50	7.04	0.38	−27.1	11	7.47	0.58	−26.3	16	6.86	0.79	−23.6	31	5.72	0.25	−26.4	15	6.77	2.33	−27.0	12
60	7.13	0.36	−26.5	15	7.63	0.55	−27.2	11	6.98	0.79	−24.2	28	5.78	0.23	−27.1	11	6.87	2.03	−26.8	13
70	7.15	0.39	−27.8	7	7.52	0.53	−27.3	10	6.94	0.89	−24.3	27	6.03	0.39	−27.0	12	7.12	1.91	−27.3	10
80	7.21	0.32	−26.8	13	7.58	0.47	−27.0	12	7.09	0.91	−23.7	31					7.13	1.67	−27.5	9
90	7.22	0.30	−27.3	10	7.75	0.57	−26.3	16	7.04	0.93	−23.6	31					7.29	1.59	−27.7	8
100	7.43	0.36	−28.2	5					6.91	0.31	−27.7	8					7.47	1.61	−28.2	5
110	7.80	0.28	−28.5	3					7.08	0.28	−29.1	0					7.43	1.51	−27.8	7
120																	7.52	1.41	−27.9	7

SOC from the FL and VFL profiles increased by approximately 3‰ and 2.2‰ with depth, respectively, while the $\delta^{13}C$ values of the SOC from the GL profile showed almost no change.

In the soils under different vegetation cover, two possible isotopic sources (C_3 and C_4 plants) of SOC were present. We calculated the proportion of SOC originated from C_3 plants (SOC_3) and from C_4 plants (SOC_4) according to the equation mentioned above section. The results (Table 2) indicated that the SOC_4 fraction was derived from the land use change to maize culture. The $\delta^{13}C$ value of the topsoil in the FL profile was higher than that of the topsoil in the VFL profile. However, the $\delta^{13}C$ value from the deepest soil in the FL profile was very similar to the value in the deepest soil layer in the VFL profile. This result indicates that the $\delta^{13}C$ values (a precursor of SOC input) were affected by the variations in land use and type following several decades of cultivation after deforestation. However, as shown in Table 2, most of the SOC was derived from the original virgin forest, with only a minority of SOC_4. The percentage of SOC_4 varied from 20% to 36% in the upper soil and was lower than 10% in the deepest soil.

Discussion

An inverse relationship was observed between soil organic matter and soil pH, with higher soil organic matter contents corresponding to lower pH values (Figs. 2 and 3). The distribution of SOC with depth was closely related to the evolution of the soil profiles (Chen *et al.*, 2005). With increasing depth, the source of organic matter gradually decreased as the period of soil formation increased. However, the SOC losses due to decomposition continuously increased with depth. Consequently, the SOC content decreased with increasing profile depth. The SOC of the topsoil showed a rapid decomposition and turnover rate due to the increased presence of microorganisms (Chen *et al.*, 2002). The SOC content decreased exponentially with depth from the highest SOC content in the topsoil (Fig. 2). In addition, the microbial population continuously decreased, and the turnover rates of SOC slowly decreased with depth in the FL profile (Fierer *et al.*, 2003). Despite the lower SOC contents with depth, the SOC was mainly composed of refractory components (below 30 cm). This result occurred because the SOC content reflects the balance between plant material inputs and organic carbon losses that result from heterotrophic decomposition (Li and Zhao, 2001). In the subtropical, monsoonal, and humid climate, the high temperatures and abundant rainfall encourage rapid vegetation growth, which results in a considerable annual input of plant debris into the soil. In Maolan, where calcium-rich limestone soils prevail, the activity of microorgan-

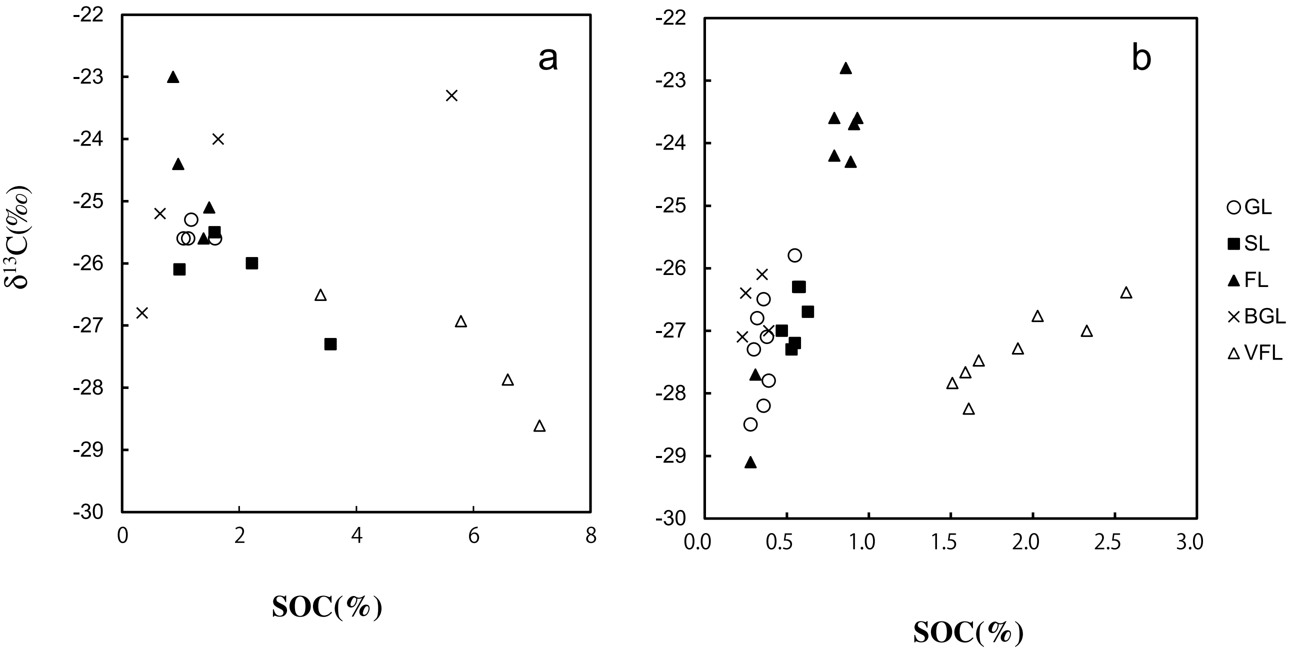

Fig. 5. SOC vs. $\delta^{13}C$ of the samples from the five soil profiles. a. SOC and $\delta^{13}C$ values from the surface of the soil profiles to a depth of 30 cm. b. SOC and $\delta^{13}C$ values from a depth of 30 cm to the bottom of the soil profiles.

isms such as bacteria and actinomycetes is very high (Office of General Survey on Soil, 1998). These microorganisms continuously decompose the organic matter to form humus. When combined, the humus and calcium ions produce polymeric and stable humus-calcium, which results in the accumulation of humus-calcium in the limestone soil (Zhu and Liu, 2006). Consequently, the SOC in the VFL profile maintained a higher SOC content than the other profiles.

In the same climate, the SOC contents and the nature of the surface vegetation are directly correlated, which significantly controls the vertical distribution of the SOC (Jobbagy and Jackson, 2000). Plant debris and root exudation are major sources of SOC under native vegetation. The net primary productivity of forest vegetation is generally higher than that of shrub vegetation (Zhu and Liu, 2006). Consequently, the rate of organic matter input into the soil is reduced when the land use changes from virgin forest to burnt grassland and farmland in Maolan areas. In contrast, the surface vegetation affects the soil texture. The topsoil of a virgin forest profile has a high SOC content and a loose soil texture (Zhu and Liu, 2006), which facilitates the downward transfer of SOC. Consequently, this uppermost layer, which has the highest SOC content, is thicker in the virgin forest profile than in the other profiles. Li and Zhao (2001) suggested that SOC levels mainly differ in the upper horizon under different land uses, especially in the upper 30 cm of the soils. In this study, the forest soil had a higher SOC content than the soils associated with other land uses. The soils under meadow and tilled lands, which represented seriously degraded land use patterns in the region, generally had the lowest organic carbon levels. The farmland soils were characterized by a slow decrease in carbon with depth and relatively low SOC levels in the topsoil. In contrast, the SOC sharply decreased in the shrub and forest soils, especially in the upper 30 cm. The grasslands and farmlands that were created from forestland experienced intensive human disturbance; consequently, the carbon losses were linked to human activities, not only in the upper 30 cm of the profiles but also at much deeper levels.

SOC is composed of several fractions that vary from very labile to refractory. The refractory organic matter fraction can have a turnover time of several hundred years, whereas the labile SOC pool has a turnover time of less than a few years (Campbell *et al*., 1967; Hsien, 1992). The distribution of organic matter among these pools is influenced by soil management practices such as crop rotation, tillage and fertilizer application. Based on these data, the turnover of SOC under the virgin forest was much slower than the turnover under the cultivated soils. Several decades after deforestation, the SOC content in the farmland soil approached a new equilibrium position. However, this equilibrium was established based on the low SOC content. In this study, some of the SOC_3 disappeared after cultivation. The remnant SOC was refractory organic matter that belonged to organo-mineral complexes, which can remain unchanged for long periods and maintain soil structure and fertility.

The $\delta^{13}C$ versus depth curves showed different profiles for the different types of vegetation cover. These differences potentially resulted from vegetation changes that occurred during profile development. From the surface soil to the base of the profiles, the $\delta^{13}C$ values of SOC were divided into two stages (Figs. 4 and 5). (1) In the first stage (from the topsoil to a depth of 30 cm), the $\delta^{13}C$ values of the SOC in GL, SL, FL, and VFL profiles increased (but not in the BGL profile). The $\delta^{13}C$ values of the SOC rapidly became enriched in ^{13}C values at a depth of 30 cm in the GL, SL, FL, and VFL profiles. This enrichment may have resulted from the fractionation effects of carbon isotopes during SOM decomposition rather than from a vegetation shift (Chen *et al*., 2002). (2) At the second stage (below the depth of 30 cm), the $\delta^{13}C$ values of the SOC slightly decreased and eventually stabilized. At the bottoms of all of the soil profiles, the $\delta^{13}C$ values of the SOC appeared to be homogeneous, and the SOM began to decompose due to the net effects of the carbon isotope fractionation.

The increasing of the $\delta^{13}C$ values with depth was related to the increasing age and degree of decay of the organic carbon (Stout *et al*., 1981; Balesdent *et al*., 1990), i.e., the increasing potentially resulted from the isotope fractionation that is associated with decay and the presence of millennia-old SOC throughout the profile, which was richer in ^{13}C than the young SOC. This finding indicates that the carbon in the deepest soils is mainly of C_3 origin, while the organic matter in the surface soil was derived from the covering vegetation litter.

The changes in the $\delta^{13}C$ values with depth have several possible explanations (Balesdent *et al*., 1990; Chen *et al*., 2002). The first explanation is the decrease in the $\delta^{13}C$ values of CO_2 or vegetation with time due to fossil fuel combustion. The second explanation involves the different decay rates of the functional group components with different $\delta^{13}C$ value. Finally, the third explanation is that the change results from real fractionation in the soil (Chen *et al*., 2002). The second and third explanations are consistent with our findings, in which the enrichment of $\delta^{13}C_{SOC}$ values resulted from the differential decay rates of the different organic matter components and the fractionation of the C isotopes during organic matter decomposition (Chen *et al*., 2002). The $\delta^{13}C$ values in the topsoil of the VFL were enriched in ^{13}C, largely due to carbon isotope fractionation, which indicated that this surface layer is the dominant source of CO_2 emissions that result from SOM decomposition.

From the surface of the soil profile to a depth of 30 cm, a clear negative linear correlation occurred between the $\delta^{13}C$ values in the SOC and the SOC contents in all but the GL and BGL profiles (Fig. 5a). Between 30 cm and the bottom of the profile, the positive correlation between the $\delta^{13}C$ values and SOC contents was well established. The variations of the $\delta^{13}C$ values in the SOC and the SOC contents with depth indicated that vegetation cover directly controlled the SOC storage. The SOC content of the topsoil mainly responds directly to the type of vegetation. In addition, the vegetation transfers organic material to deeper portions of the soil profile.

Conclusions

We measured the SOC contents and their $\delta^{13}C$ values of bulk soil samples that were collected at five sites in the karst area of Southwest China, where had a different vegetation cover. Variations in the $\delta^{13}C$ values and decreases in the SOC contents with depth were well correlated. A distinct difference was observed in the vertical patterns of the stable carbon isotopic compositions of the SOC in these profiles. This difference potentially reflects site-specific factors, such as soil type, vegetation cover, and soil pH, which control the different organic component contents that comprise SOC and the soil carbon turnover rates in the profiles. The vertical patterns of stable carbon isotopic composition in this study region differed according to the type of vegetation cover. Topsoil is susceptible to variations in vegetation cover and is the main element of a soil profile that reflects the weathering of the underlying bedrock. Vegetation cover facilitates the transport of larger amounts of organic matter to greater depths in the soil profile.

Previous studies have paid little attention to the effects of vegetation cover on karst processes. This research was based on a relatively small, but typical and representative area, in which the most common forms of land use were represented. This study showed clear interrelationships between the types of vegetation cover and the characteristics of soil organic matter in a typical karst forest area. The SOC concentration changed according to the extent of human interference in the natural soil profile. A better understanding of the soil carbon distributions and concentrations under a variety of land uses could be useful for estimating recent and future releases of sequestered soil carbon. We believe that our results make a significant contribution to the protection of fragile karst soil resources and the readjustment of the land use structure in Southwest China.

Acknowledgments—The authors thank the two anonymous reviewers whose comments and suggestions greatly improved the quality of this manuscript. This work was supported jointly by the Chinese National Natural Science Foundation (No. 41325010), National Key Basic Research Program of China (No. 2013CB956703) and the Fundamental Research Funds for the Central Universities (No. 2652013055).

References

Balesdent, J., Mariotti, A. and Boisgontier, D. (1990) Effect of tillage on soil organic carbon mineralization estimated from $\delta^{13}C$. *J. Soil Sci*. **41**, 587–596.

Biedenbender, S. H., McClaran, M. P., Quade, J. and Weltz, M. A. (2004) Landscape patterns of vegetation change indicated by soil carbon isotope composition. *Geoderma* **119**, 69–83.

Boutton, T. W., Wong, W. W., Hachey, D. L., Lee, L. S., Cabrera, M. P. and Klein, P. G. (1983) Comparison of quartz and pyrex tubes for combustion of organic samples for stable carbon isotope analysis. *Anal. Chem*., **55**, 1832–1833.

Boutton, T. W., Archer, S. R., Midwood, A. J., Zitzer, S. F. and Bol, R. (1998) $\delta^{13}C$ values of soil organic carbon and their use in documenting vegetation change in a subtropical savanna ecosystem. *Geoderma* **82**, 5–41.

Calvin, M. and Benson, A. A. (1948) The path of carbon in photosynthesis. *Science* **107**, 476–480.

Campbell, C. A., Paul, E. A., Rennie, D. A. and McCallum, K. J. (1967) Applicability of the carbon-dating method of analysis to soil humus studies. *Soil Sci*. **104**, 217–224.

Chen, Q. Q., Shen, C. D., Peng, S. L., Sun, Y. M., Yi, W. X., Li, Z. A. and Jiang, M. T. (2002) Soil organic matter turnover in the subtropical mountainous region of South China. *Soil Sci*. **167**, 401–415.

Chen, Q. Q., Shen, C. D., Sun, Y. M., Peng, S. L., Yi, W. X., Li, Z. A. and Jiang, M. T. (2005) Spatial and temporal distribution of carbon isotopes in soil organic matter at the Dinghushan Biosphere Reserve, South China. *Plant and Soil* **273**, 115–128.

Farquhar, G. D., Ehleringer, J. R. and Hubick, K. Y. (1989) Carbon isotope discrimination and photosynthesis. *Ann. Rev. Plant Mol. Biol*. **40**, 503–537.

Feng, X. J., Simpson, A. J., Gregorich, E. G., Elberling, B., Hopkins, D. W., Sparrow, A. D., Novis, P. M., Greenfield, L. G. and Simpson, M. J. (2010) Chemical characterization of microbial-dominated soil organic matter in the Garwood Valley, Antarctica. *Geochim. Cosmochim. Acta* **74**, 6485–6498.

Fierer, N., Schmiel, J. P. and Holden, P. A. (2003) Variations in microbial community composition through two soil depth profiles. *Soil Biol. Biochem*. **35**, 167–176.

Hatch, M. D. and Slack, C. R. (1970) The C_4 carboxylic acid pathway of photosynthesis. *Progress in Phytochemistry* (Reinhold, L. and Liwschitz, Y., eds.), 35–106, Wiley-Interscience.

Hsien, Y. P. (1992) Pool size and mean age of stable soil organic carbon in cropland. *Soil Sci. Soc. Am. J*. **56**, 460–464.

Jobbagy, E. G. and Jackson, R. B. (2000) The vertical distribution of soil organic carbon and its relation to climate and vegetation. *Ecol. Appl*. **10**, 423–436.

Li, W., Yu, L., Yuan, D., Xu, H. and Yang, Y. (2004). Bacteria biomass and carbonic anhydrase activity in some karst areas of southwest China. *J. Asian Earth Sci*. **24**, 145–152.

Li, Y. Q. and Mathews, B. W. (2010) Effect of conversion of sugarcane plantation to forest and pasture on soil carbon in Hawaii. *Plant and Soil* **335**, 245–253.

Li, Z. and Zhao, Q. (2001) Organic carbon content and distribution in soils under different land uses in tropical and subtropical China. *Plant and Soil* **231**, 175–185.

Liu, G. S., Jiang, N., Zhang, L. and Liu, Z. (1996) *Soil Physical and Chemical Analysis and Description of Soil Profiles*. 24–25, China Standards Press.

Malhi, Y., Baldocchi, D. D. and Jarvis, P. G. (1999) The carbon balance of tropical, temperate and boreal forests. *Plant Cell Environ*. **22**, 517–523.

Midwood, A. J. and Boutton, T. W. (1998) Soil carbonated decomposition by acid has little effect on $\delta^{13}C$ of organic matter. *Soil Biol. Biochem*. **30**, 1301–1307.

Office of General Survey on Soil (1998) *China Soil*. 150–153, Agricultural Publishing House of China, Beijing.

Piao, H., Liu, Q., Yu, D., Guo, J. and Ran, J. (2001) Origins of soil organic carbon with the method of natural $\delta^{13}C$ abundance in maize fields. *Acta Ecol. Sinica* **21**, 434–439 (in Chinese with English abstract).

Raich, J. W. and Potter, C. S. (1995) Global patterns of carbon dioxide emissions from soils. *Global Biogeochem. Cycles* **9**, 23–36.

Resh, S. G., Binkley, D. and Parrotta, J. A. (2002) Greater soil carbon sequestration under nitrogen-fixing trees compared with Eucalyptus Species. *Ecosystems* **5**, 217–231.

Schlesinger, W. H. (1977) Carbon balance in terrestrial detritus. *Annu. Rev. Ecol. Syst*. **8**, 51–81.

Staddon, P. L. (2004) Carbon isotopes in functional soil ecology. *Trends Ecol. Evol*. **19**, 148–154.

Stout, J. D., Gob, K. M. and Rafter, T. A. (1981) Chemistry and turnover of naturally occurring resistant organic compounds in soil. *Soil Biochemistry* (Paul, E. A. and Ladd, J. N., eds.), **5**, 1–73, Marcel Dekker Inc.

Trumbore, S. E., Chadwich, O. A. and Amundson, R. (1996) Rapid exchange between soil carbon and atmospheric carbon dioxide driver by temperature change. *Science* **272**, 393–396.

Vagen, T.-G., Markus, G. W. and Keith, D. S. (2006) Stable isotopes for characterisation of trends in soil carbon following deforestation and land use change in the highlands of Madagascar. *Geoderma* **135**, 133–139.

Wang, S. J., Ji, H. B., Ziyuan, O. Y., Zhou, D. Q., Zhen, L. P. and Li, T. Y. (1999) Preliminary study on weathering and pedogenesis of carbonate rock. *Sci. China Ser*. **D42**, 572–581.

Woodwell, G. M., Mackenzie, R. A., Houghton, R. A., Apps, M., Gorham, E. and Davidson, E. (1998) Biotic feedbacks in the warming of the Earth. *Climatic Change* **40**, 495–518.

Yuan, D. (1997) The carbon cycle in the karst. *Z. Geomorphol*. **108**, 91–102.

Zhang, C. and Yuan, D. (2004) Hydrochemical variation of typical karst subterranean stream basin and its relationship with landuse change. *J. Soil Water Conserv*. **18**, 134–137.

Zhu, S. and Liu, C.-Q. (2006) Vertical patterns of stable carbon isotope in soils and particle-size fractions of karst areas, Southwest China. *Environ. Geol*. **50**, 1119–1127.